International Journal of Heat and Mass Transfer 209 (2023) 124109

Contents lists available at ScienceDirect

International Journal of Heat and Mass Transfer

journal homepage: www.elsevier.com/locate/hmt

Steady state thermal analysis of a porous fin with radially outwards fluid flow

Ankur Jain*, Muhammad M. Abbas, Mohsen Torabi

Mechanical and Aerospace Engineering Department, University of Texas at Arlington, Arlington, TX, USA

ARTICLE INFO

Article history:
Received 7 February 2023
Revised 8 March 2023
Accepted 15 March 2023
Available online 29 March 2023

Keywords:
Fins
Porous medium
Heat transfer enhancement
Fin effectiveness
Thermal Management

ABSTRACT

Fins are used ubiquitously in engineering devices and systems for enhancement of heat transfer and energy storage. While traditional fins are made of non-porous materials, porous fins with natural convection porous flow orthogonal to the fin direction have also been studied. In contrast to these, there is a lack of work on porous fins in which the fluid flow may be along the direction of the fin. In such a fin, porosity may increase advective heat removal due to increased flow rate but may also impede conductive heat removal due to reduction in effective thermal conductivity. Due to these competing trade-offs, there is a need for comprehensive analysis of thermal performance of such a porous fin. This work derives a solution for the steady-state temperature distribution in a porous fin with advection along the fin direction. It is shown that temperature distribution in such a porous fin is governed by a convection-diffusion-reaction equation. A solution for the temperature distribution is derived in the form of modified Bessel functions of non-zero order. Two distinct fin performance parameters are defined and derived in order to characterize porous fin performance. It is found that thermal properties of the fin as well as ambient convective conditions strongly impact the relationship between fin porosity and fin performance. While in some cases, it is found that an optimum porosity exists that maximizes heat removal, in other cases, the use of a porous fin is found to be not desirable at all. The analysis presented here helps fully understand these trade-offs, and provides useful guidelines for porous fin design for maximum heat removal.

1. Introduction

Fins are used commonly in a wide variety of engineering problems for enhanced heat transfer and energy storage [1,2]. Common applications include thermal management of engines and microelectronics [3], improvement in rate of phase change energy storage [4] and heat transfer enhancement in heat exchangers [2]. The fin effect also appears in bioheat transfer [5]. When a well-designed fin is placed over a hot base surface, the reduction in heat transfer to the ambient due to reduced direct contact with the hot surface may be overcome by the additional heat transfer through the fin, thereby providing an improvement in overall heat transfer. Fin performance is often characterized by parameters such as fin effectiveness and fin efficiency [1,2]. While the fin effectiveness refers to heat removal rate by the fin relative to heat removal in the absence of any fin at all, fin efficiency refers to the heat removal rate by the fin relative to the best possible fin that is isothermal at the base temperature. While the fin efficiency is, by definition, always less than one, the effectiveness of a fin must be greater than one in order to justify the use of the fin.

Fins are most commonly made of solid materials such as metals, although the use of porous fins, which offer reduced fin weight, among other possible advantages, has also been investigated. Porous metal fins are of particular interest for electronics cooling [6]. Heat transfer enhancement in a porous fin occurs due to additional heat removed by the porous fluid flow [7]. For example, vertical infiltration of a horizontal fin by buoyant fluid flow from the ambient results in an additional, non-linear sink term in the energy conservation equation [7,8], which has been shown to improve fin performance. Buoyancy-driven porous flow in such fins is often modeled on the basis of the Darcy law [9,10] and the Boussinesq approximation [11]. The energy equation governing the natural convection porous fin is non-linear. A number of analytical techniques such as homotopy perturbation method [12] and differential transformation method [8] have been used for determining the temperature distribution, and, subsequently, the fin performance characteristics. A number of numerical techniques [13,14] have been proposed as well. The effects of natural convection [15] as well as radiation [16] in a porous fin have been accounted for. Performance of porous fins of various shapes and sizes has been characterized [17,18], and fin optimization has been

* Corresponding author: Ankur Jain, 500 W First St, Rm 211, Arlington, TX, USA, 76019
E-mail address: jaina@uta.edu (A. Jain).

https://doi.org/10.1016/j.ijheatmasstransfer.2023.124109
0017-9310/

Nomenclature

$\bar{A}$	Péclet number
$\bar{B}$	ratio of convective heat removal and diffusion terms
Bi_{tip}	Biot number at the fin tip
c_f	fluid heat capacity ($Jkg^{-1}K^{-1}$)
h	convective heat transfer coefficient around the fin ($Wm^{-2}K^{-1}$)
h_{tip}	convective heat transfer coefficient at the fin tip ($Wm^{-2}K^{-1}$)
k_{eff}	effective thermal conductivity ($Wm^{-1}K^{-1}$)
k_f	fluid thermal conductivity ($Wm^{-1}K^{-1}$)
k_s	solid thermal conductivity ($Wm^{-1}K^{-1}$)
L	fin radial length (m)
$\bar{L}$	non-dimensional fin radial length
r	radial coordinate (m)
R_0	fin base radius (m)
T	temperature (m)
T_∞	ambient temperature around the fin (K)
$T_{\infty,tip}$	ambient temperature at the fin tip (K)
T_b	fin base temperature (K)
U	velocity (m)
w	fin height (m)
$\bar{w}$	non-dimensional fin height
Δp	pressure difference (Pa)
K	permeability (m^2)
μ	viscosity ($kgm^{-1}s^{-1}$)
ϕ	porosity
ρ_f	fluid density (kgm^{-3})
θ	non-dimensinal temperature
$\theta_{\infty,tip}$	non-dimensional ambient temperature at the fin tip
ξ	non-dimensional radial coordinate

carried out [19]. Comparison of fin performance with the baseline solid fin has also been carried out [20]. Other, more complicated considerations, such as temperature-dependent heat generation [21] or thermal properties [22] have also been analyzed.

Most of the literature on porous fins assumes a horizontal fin, through which, buoyancy-driven vertical cross-flow of the surrounding fluid occurs, which results in heat removal from the fin. However, other porous fin configurations may also be possible that result in enhanced heat transfer. For example, it is possible for porous fluid flow between the base of the fin and the tip of the fin along the fin direction, as opposed to across the fin direction. This could be driven, for example, by an imposed pressure difference between the fin base and tip. Such a pressure-driven flow may be a lot more effective in heat removal than the natural convection driven cross-flow considered in most of the past literature on porous fin heat transfer [7,8,12,13]. An illustrative example of this scenario is presented in Fig. 1(a) that shows a radial fin connected to a base cylinder, where, a pressure gradient driven porous fluid flow is established in the radially outward direction, provided that the is sealed to prevent any fluid leakage on the lateral surface. In such a case, heat removal from the base cylinder by the radial fin occurs due to two mechanisms acting in parallel – thermal conduction down the porous fin material, governed by the effective thermal conductivity of the porous fin, and advection of heat by the porous fluid flow from the hot base of the fin to the relatively cooler tip of the fin. The conductive and advective heat transport mechanisms are likely to be influenced very differently by the fin porosity. For example, increased porosity in the fin material likely reduces conductive heat removal due to reduction in effective thermal conductivity [10]. On the other hand, increased porosity likely improves porous fluid flow rate by increasing the pore area through which the fluid can flow [9], thereby improving the advective removal of heat. Due to these opposing effects, it is of much interest to carry out heat transfer analysis of the porous fin considered here with radially outwards pressure-driven fluid flow. Primary interests in such analysis include the derivation of the temperature distribution and fin performance parameters, identification of key non-dimensional numbers that govern this problem and development of an understanding of how the two thermal transport mechanisms – conductive and advective – are affected by properties of the porous material and other problem parameters. It is of much practical importance to determine under what conditions is the use of a porous fin beneficial, and when so, whether there exists an optimal value of the porosity due to competing trade-offs between conductive and advective heat removal. Such an optimization may help design a porous fin to deliver the best possible thermal performance under given conditions. Unfortunately, the analytical tools that have been developed for studying convective porous fin with natural convection driven flow across the fin direction [7,8] or for optimizing non-porous fins [23,24] are not readily translatable to study this problem, for which, the governing energy equation applicable to the present problem must be formulated and solved.

This work presents theoretical heat transfer analysis of a porous fin with radially outwards porous flow driven by a pressure gradient. It is shown that the temperature field of the fin is governed by a convection-diffusion-reaction (CDR) equation containing certain non-dimensional parameters. A solution of this equation is used to characterize the fin performance parameters, and, in particular, the impact of porosity on fin performance. A number of special cases of the analysis are also considered. This work presents new insights into porous fin theory, which may be helpful in the design of porous fins for enhanced heat removal.

2. Problem Definition

The problem of interest in this work pertains to heat removal from the outer wall of a hot cylindrical body by a radial fin. The fin is made of a porous material that permits radially outwards fluid flow from the wall towards the tip, as shown schematically in Fig. 1(a). The lateral surfaces of the fin are assumed to be sealed, so that only radially outwards porous flow is possible. The hot cylindrical body is assumed to be hollow and thin walled, and carrying a fluid within, so that a pressure difference between the inside of the cylindrical body and the tip of the fin results in radially outwards fluid flow through the fin material.

Heat transfer in the porous fin described above occurs both due to diffusion in the solid and due to advection by fluid flow through the pores of the porous material. This is in contrast with traditional non-porous fins, in which diffusion is the only heat transfer mechanism within the fin. Note that the radial porous fin configuration being analyzed here is distinct from previously studied porous fin configurations, in which, buoyancy-driven fluid flow occurs in a direction orthogonal to the fin direction [7,8,12,13], as opposed to advection-driven flow along the fin in the present work.

The interest here is to derive expressions for the steady state temperature distribution in the porous fin and thus determine its heat transfer performance. Understanding the contributions of diffusion and advection towards overall heat removal may help identify scenarios where such a porous fin may be particularly effective or ineffective.

The inner and outer radii of the fin are R_0 and R_0+L, where L is the fin length. The height of the fin is w. Uniform porosity and permeability of the fin material are denoted by ϕ and K, respectively. Thermal conductivity, density and heat capacity of the fluid are taken to be k_f, ρ_f and c_f, respectively. A similar nomenclature is followed for solid component of the fin, with subscript s.

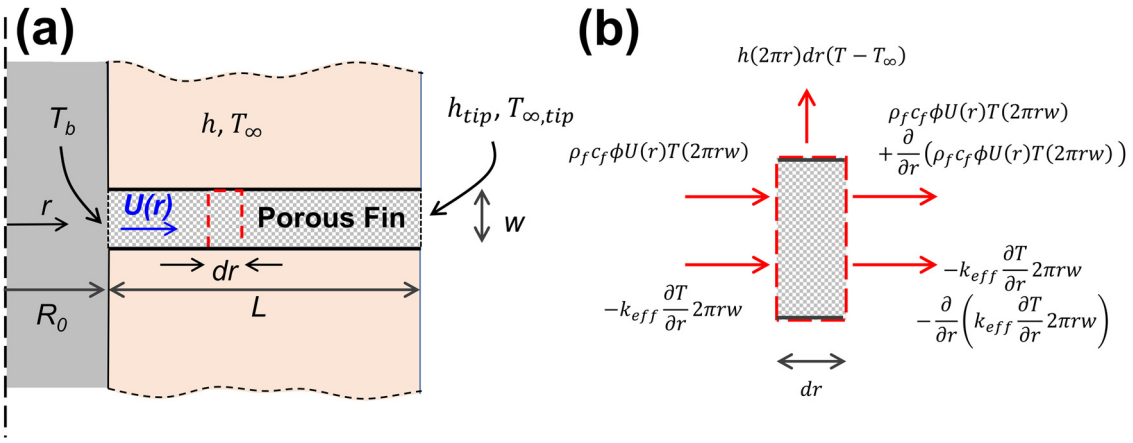

Fig. 1. (a) Schematic of the geometry of a porous radial fin with outwards, pressure-driven flow through the pores of the fin material, (b) Schematic of energy balance for an infinitesimal element of the porous fin, showing advective and diffusive transport through the fin as well as convective heat loss to the surrounding medium.

Fluid viscosity is denoted by μ. The effective thermal conductivity of the porous medium is taken to be k_{eff}. The pressure difference between the base (r=R_0) and tip (r=R_0+L) of the fin is taken to be Δp. Temperature at the base of the fin is denoted by T_b. Freestream temperature of the medium surrounding the fin is taken to be T_∞. Thermal interactions between the outer surface of the fin and the surrounding ambient are assumed to be represented by a convective heat transfer coefficient h. In addition, a convective heat transfer coefficient h_{tip} along with an external freestream temperature $T_{\infty,tip}$ is assumed at the tip of the fin. Note that in many cases, $T_{\infty,tip} = T_\infty$, although this assumption is not needed/made in this work.

A number of other assumptions are made in order to carry out a thermal analysis of a porous fin. Axisymmetry of the temperature field is assumed. The velocity field is assumed to be only radial, as the fin surfaces are sealed to prevent fluid leakage normal to the fin direction. All transport properties are assumed to be independent of temperature. Radiative heat transfer and natural convection effects around the fin are neglected, due to a reasonably small temperature difference between the fin base and ambient. Note that radiative effects may be modeled approximately by an effective heat transfer coefficient [25], but this is not investigated in detail in the present work. The porous flow is assumed to be Newtonian and laminar, and, therefore, governed by the Darcy equation. A constant permeability is assumed. Based on these assumptions, a governing differential equation for the radial temperature distribution in the porous fin may be derived by considering energy conservation in an infinitesimal element at radial location r and of radial dimension dr. As shown in Fig. 1(b), thermal energy flows in and out of this element include thermal conduction, advection due to radial fluid flow and heat loss/gain from the ambient due to the imposed convective heat transfer coefficient. By carrying out a balance between these energy flow terms in steady state, the following governing energy equation may be derived [1,2]:

$$\frac{k_{eff}}{r}\frac{\partial}{\partial r}\left(r\frac{\partial T}{\partial r}\right) - \frac{\phi\rho_f c_f}{r}\frac{\partial}{\partial r}(r\cdot T\cdot U) - \frac{h}{w}(T-T_\infty) = 0 \tag{1}$$

where $T(r)$ and $U(r)$ are the temperature and velocity fields, respectively, within the porous fin. k_{eff} is the effective thermal conductivity of the medium that accounts for thermal conduction through both solid and fluid constituents. Compared to the standard fin equation [1], Eq. (1) contains an additional term that models advective thermal transport.

Appendix A shows that, based on the Darcy equation for porous flow in radial coordinates, the radial velocity field in the porous fin is given by

$$U(r) = \frac{K\cdot\Delta p}{\mu\cdot\ln\left(\frac{R_0+L}{R_0}\right)\cdot r} \tag{2}$$

The $1/r$ dependence of the velocity field above is consistent with the requirement of mass conservation as the fluid flows radially outwards.

The two boundary conditions associated with Eq. (1) are

$$T = T_b \qquad (r = R_0) \tag{3}$$

$$-k_{eff}\frac{\partial T}{\partial r} = h_{tip}\left(T - T_{\infty,tip}\right) \qquad (r = R_0 + L) \tag{4}$$

The following non-dimensional variables and parameters are introduced:

$$\xi = \frac{r}{R_0};\ \theta = \frac{T-T_\infty}{T_b-T_\infty};\ \bar{A} = \frac{\mathrm{K}\cdot\rho_f c_f\cdot\Delta p\cdot\phi}{\mu\cdot\ln\left(\frac{R_0+L}{R_0}\right)k_{eff}};\ \bar{B} = \frac{hR_0^2}{k_{eff}w};\ \bar{L} = \frac{L}{R_0};$$
$$Bi_{tip} = \frac{h_{tip}R_0}{k_{eff}};\ \theta_{\infty,tip} = \frac{T_{\infty,tip}-T_\infty}{T_b-T_\infty};\ \bar{w} = \frac{w}{R_0} \tag{5}$$

Note that based on definitions above, $\bar{A}$ may be interpreted as the ratio of advective and diffusive transport, i.e., a Péclet number [10]. Similarly, $\bar{B}$ is the ratio of the term representing heat removal to the ambient and diffusive thermal transport term [1,26], similar to the Damköhler number that appears in mass transfer problems [27].

Inserting the form of the velocity field from Appendix A as well as the non-dimensional variables from Eq. (5) into the governing equation given by Eq. (1) results in the following non-dimensional governing energy conservation for the temperature field in the fin

$$\frac{1}{\xi}\frac{\partial}{\partial\xi}\left(\xi\frac{\partial\theta}{\partial\xi}\right) - \frac{\bar{A}}{\xi}\frac{\partial\theta}{\partial\xi} - \bar{B}\theta = 0 \tag{6}$$

This is a Convection-Diffusion-Reaction (CDR) equation that appears in several other heat and mass transfer problems including drug delivery [26], reactor engineering [28] and pollution dispersion problems [29]. The non-dimensional boundary conditions associated with this equation are given by

$$\theta = 1 \qquad (\xi = 1) \tag{7}$$

$$-\frac{\partial\theta}{\partial\xi} = Bi_{tip}\left(\theta - \theta_{\infty,tip}\right) \qquad \left(\xi = 1 + \bar{L}\right) \tag{8}$$

3. Solution of the Problem

In order to solve Eq. (6), one may substitute $\theta(\xi) = \xi^{\bar{A}/2}\phi(\xi)$, which can be shown to result in the following equation for ϕ:

$$\xi^2 \frac{\partial^2 \phi}{\partial \xi^2} + \xi \frac{\partial \phi}{\partial \xi} - \left(\bar{B}\xi^2 + \frac{\bar{A}^2}{4}\right)\phi = 0 \tag{9}$$

which is the modified Bessel equation [30]. Therefore, a solution for the temperature distribution may be written as

$$\theta(\xi) = \xi^{\bar{A}/2}\left[c_1 I_{\bar{A}/2}(\sqrt{\bar{B}}\xi) + c_2 K_{\bar{A}/2}(\sqrt{\bar{B}}\xi)\right] \tag{10}$$

where I and K refer to modified Bessel functions of the first and second kind, respectively. $\bar{A}/2$ is the order of the modified Bessel functions. Note that by definition, $\bar{B} > 0$. c_1 and c_2 are constants to be determined from the boundary conditions.

Inserting Eq. (10) into the boundary conditions given by Eqs. (7) and (8) results in the following two linear algebraic equations in c_1 and c_2.

$$c_1 I_{\bar{A}/2}(\sqrt{\bar{B}}) + c_2 K_{\bar{A}/2}(\sqrt{\bar{B}}) = 1 \tag{11}$$

$$\begin{aligned}\left(1+\bar{L}\right)^{\bar{A}/2}\Bigg[\sqrt{\bar{B}}\Big(c_1 I_{\frac{\bar{A}}{2}-1}\Big(\sqrt{\bar{B}}\big(1+\bar{L}\big)\Big) - c_2 K_{\frac{\bar{A}}{2}-1}\Big(\sqrt{\bar{B}}\big(1+\bar{L}\big)\Big)\Big) \\ + Bi_{tip}\Big(c_1 I_{\frac{\bar{A}}{2}}\Big(\sqrt{\bar{B}}\big(1+\bar{L}\big)\Big) + c_2 K_{\frac{\bar{A}}{2}}\Big(\sqrt{\bar{B}}\big(1+\bar{L}\big)\Big)\Big)\Bigg] = Bi_{tip}\theta_{\infty,tip}\end{aligned} \tag{12}$$

from where, c_1 and c_2 may be determined as follows

$$c_1 = \frac{-\sqrt{\bar{B}}K_{\frac{\bar{A}}{2}-1}\Big(\sqrt{\bar{B}}\big(1+\bar{L}\big)\Big) + Bi_{tip}K_{\frac{\bar{A}}{2}}\Big(\sqrt{\bar{B}}\big(1+\bar{L}\big)\Big) - \theta_{\infty,tip}Bi_{tip}\big(1+\bar{L}\big)^{-\frac{\bar{A}}{2}}K_{\frac{\bar{A}}{2}}\Big(\sqrt{\bar{B}}\Big)}{-\sqrt{\bar{B}}\Big(K_{\frac{\bar{A}}{2}-1}\Big(\sqrt{\bar{B}}\big(1+\bar{L}\big)\Big)I_{\frac{\bar{A}}{2}}\Big(\sqrt{\bar{B}}\Big) + I_{\frac{\bar{A}}{2}-1}\Big(\sqrt{\bar{B}}\big(1+\bar{L}\big)\Big)K_{\frac{\bar{A}}{2}}\Big(\sqrt{\bar{B}}\Big)\Big) + Bi_{tip}\Big(K_{\frac{\bar{A}}{2}}\Big(\sqrt{\bar{B}}\big(1+\bar{L}\big)\Big)I_{\frac{\bar{A}}{2}}\Big(\sqrt{\bar{B}}\Big) - I_{\frac{\bar{A}}{2}}\Big(\sqrt{\bar{B}}\big(1+\bar{L}\big)\Big)K_{\frac{\bar{A}}{2}}\Big(\sqrt{\bar{B}}\Big)\Big)} \tag{13}$$

and

$$c_2 = \frac{\sqrt{\bar{B}}I_{\frac{\bar{A}}{2}-1}\Big(\sqrt{\bar{B}}\big(1+\bar{L}\big)\Big) + Bi_{tip}I_{\frac{\bar{A}}{2}}\Big(\sqrt{\bar{B}}\big(1+\bar{L}\big)\Big) - \theta_{\infty,tip}Bi_{tip}\big(1+\bar{L}\big)^{-\frac{\bar{A}}{2}}I_{\frac{\bar{A}}{2}}\Big(\sqrt{\bar{B}}\Big)}{\sqrt{\bar{B}}\Big(I_{\frac{\bar{A}}{2}-1}\Big(\sqrt{\bar{B}}\big(1+\bar{L}\big)\Big)K_{\frac{\bar{A}}{2}}\Big(\sqrt{\bar{B}}\Big) + K_{\frac{\bar{A}}{2}-1}\Big(\sqrt{\bar{B}}\big(1+\bar{L}\big)\Big)I_{\frac{\bar{A}}{2}}\Big(\sqrt{\bar{B}}\Big)\Big) + Bi_{tip}\Big(I_{\frac{\bar{A}}{2}}\Big(\sqrt{\bar{B}}\big(1+\bar{L}\big)\Big)K_{\frac{\bar{A}}{2}}\Big(\sqrt{\bar{B}}\Big) - K_{\frac{\bar{A}}{2}}\Big(\sqrt{\bar{B}}\big(1+\bar{L}\big)\Big)I_{\frac{\bar{A}}{2}}\Big(\sqrt{\bar{B}}\Big)\Big)} \tag{14}$$

This completes the solution for the fin temperature field.

Note that the effective thermal conductivity k_{eff} appearing in Eq. (1) combines thermal conduction in both solid and fluid constituents of the porous fin. In general, k_{eff} depends on the porosity of the medium [10]. Depending on the nature of the porous material, a number of theoretical models are available to compute k_{eff} [10]. In the present work, the weighted average model is used as follows:

$$k_{\text{eff}} = (1-\phi)k_s + \phi k_f \tag{15}$$

where k_s and k_f are the thermal conductivities of the solid and fluid, respectively.

In order to help understand the relative role of advective and conductive heat removal mechanisms, as well as the influence of various problem parameters, heat transfer in this problem may be represented approximately by a thermal resistance network of the porous fin shown in Fig. 2. Heat from the base is removed by the fin through conduction and advection, which are distinct mechanisms that operate in parallel as represented by the resistances R_{cond} and R_{adv} in Fig. 2. Heat transported conductively through the fin is eventually transferred to the ambient either through the outer surface of the fin (R_{surf}), or, in parallel, through the fin tip (R_{tip}). In case heat transfer through the fin tip is negligible, for example, in case of a very long fin, R_{tip} may be omitted from the resistance network in Fig. 2.

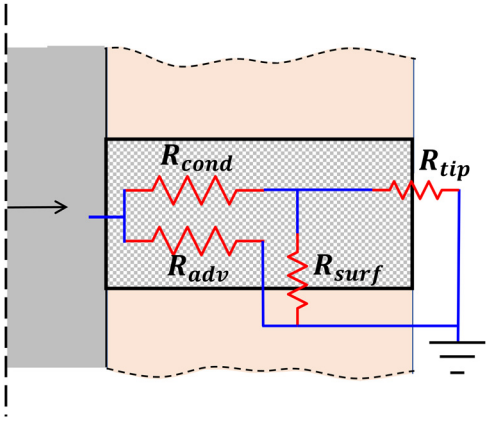

Fig. 2. An approximate schematic of the thermal resistance network of the porous fin showing conductive and advective heat removal from the base, as well as dissipation into the ambient through the fin surface and fin tip.

4. Fin Performance Parameters

A number of performance parameters are commonly used to compare the rate of heat removal by the fin with idealized and baseline cases [1]. In the present porous fin analysis, two specific cases are of interest. Firstly, performance of the porous fin may be compared with a baseline case with no fin at all, in which case, heat removal occurs purely due to convective heat transfer directly from the base of the fin into the ambient. Another interesting comparison is between heat removal by the porous fin and by a comparable non-porous fin. This may help understand the impact of porosity of the fin material and subsequent pressure-driven flow on heat removal.

In order to carry out such comparisons, the heat removal rate from the porous fin must be determined first. Heat is removed from the base of the fin due to both diffusion and advection. Thus, the heat removal rate may be written as

$$q = \left(-k_{eff}\left(\frac{\partial T}{\partial r}\right)_{r=R_0} + \phi\rho_f c_f \cdot \mathrm{U}(R_0)(T_b - T_\infty)\right)2\pi R_0 w \tag{16}$$

Thus, a non-dimensional heat removal rate may be defined as follows

$$\begin{aligned}\bar{q} = \frac{q}{k_{eff}(T_b - T_\infty)2\pi w} = -\left(\frac{\partial\theta}{\partial\xi}\right)_{\xi=1} \\ + \bar{A} = -\sqrt{\bar{B}}\Big(c_1 I_{\frac{\bar{A}}{2}-1}\Big(\sqrt{\bar{B}}\Big) - c_2 K_{\frac{\bar{A}}{2}-1}\Big(\sqrt{\bar{B}}\Big)\Big) + \bar{A}\end{aligned} \tag{17}$$

where the first and second terms represent conductive and advective heat transfer rates, respectively.

4.1. Comparison with no fin case

The ratio of heat removed by the fin and heat removed without the fin is usually referred to as the fin effectiveness [1]. In the present case, the rate of heat removed without the fin is simply $h(T_b - T_\infty)2\pi R_0 w$. Using this in conjunction with Eq. (16), the following expression for fin effectiveness may be obtained

$$\eta = \frac{1}{\bar{w}\bar{B}}\left(-\left(\frac{\partial\theta}{\partial\xi}\right)_{\xi=1} + \bar{A}\right) = \frac{1}{\bar{w}\bar{B}}\left(\bar{A} - \sqrt{\bar{B}}\left(c_1 I_{\frac{\bar{A}}{2}-1}\left(\sqrt{\bar{B}}\right) - c_2 K_{\frac{\bar{A}}{2}-1}\left(\sqrt{\bar{B}}\right)\right)\right) \tag{18}$$

For a well-designed fin, η must be larger than one, since the fin is expected to remove more heat than would be removed without it.

4.2. Comparison with non-porous fin case

In order to quantify the benefit of porous flow in the fin, one may define a porous fin effectiveness, η_{porous} by comparing the heat removed by the porous fin with heat removed by a comparable non-porous fin of the same dimensions and in the same conditions. η_{porous} quantifies whether it is beneficial to replace a solid fin with a porous fin under the same operating conditions. On one hand, compared to the non-porous fin, the porous fin offers greater heat removal due to advection along with the radially outwards porous fluid flow. However, it may also suffer from reduced heat removal by conduction down the fin due to the expected reduction in effective thermal conductivity of the fin compared to that of the baseline non-porous fin.

In order to understand which of these effects may dominate, one may compute the heat removed by a non-porous fin using the results presented here, but with $\bar{A} = 0$ and using thermal conductivity of the solid material instead of the effective thermal conductivity. By doing so, the following expression for the porous fin effectiveness may be derived

$$\eta_{porous} = \frac{k_{eff}}{k_s}\frac{\bar{A} - \sqrt{\bar{B}}\left(c_1 I_{\frac{\bar{A}}{2}-1}\left(\sqrt{\bar{B}}\right) - c_2 K_{\frac{\bar{A}}{2}-1}\left(\sqrt{\bar{B}}\right)\right)}{-\sqrt{\bar{B}_s}\left(c_{1,s} I_1\left(\sqrt{\bar{B}_s}\right) - c_{2,s} K_1\left(\sqrt{\bar{B}_s}\right)\right)} \tag{19}$$

where $\bar{B}_s = \frac{hR_0^2}{k_s w}$ and k_s refers to thermal conductivity of the solid material. The coefficients $c_{1,s}$ and $c_{2,s}$ are obtained from the boundary conditions corresponding to the zero-advection non-porous fin problem, i.e., by setting $\bar{A} = 0$ and $\bar{B} = \bar{B}_s$ in Eqs. (13) and (14).

η and η_{porous} defined above are important fin performance metrics that characterize how well the porous fin performs compared to cases without a fin at all and with a comparable but non-porous fin. While η represents how well the porous fin performs compared to no fin at all, η_{porous} governs whether the porous fin is better than an equivalent non-porous fin. These parameters also help understand the impact of various problem parameters, such as porosity on fin performance.

5. Special Cases

5.1. Special cases for transport conditions

The general problem solved in Section 3 accounts for both conduction and advection driven heat transfer down the fin. While both mechanisms may be important in general, two special cases in which one or the other mechanism dominates may be of interest in specific applications.

5.1.1. Negligible diffusion

In certain cases, diffusion may be negligible compared to advection, for example when the flow velocity is relatively large. In order to model this special case, the first term on the left hand of the governing equation, given by Eq. (6) may be neglected. This results in the following simplified governing equation

$$\frac{\bar{A}}{\xi}\frac{\partial\theta}{\partial\xi} + \bar{B}\theta = 0 \tag{20}$$

As expected, in the absence of diffusion, the governing equation becomes a first-order differential equation, for which, only the upstream boundary condition ($\theta = 1$ at $\xi = 0$) is needed. The solution for the temperature distribution in the fin is given by

$$\theta(\xi) = \exp\left(-\frac{\bar{B}}{\bar{A}}\xi^2\right) \tag{21}$$

which is indeed the solution for a pure-advection problem [25].

Note that $\bar{B}/\bar{A} = \frac{hR_0^2 \cdot \mu \cdot \ln(\frac{R_0+L}{R_0})}{K \cdot \rho_f c_f \cdot \Delta p \cdot \phi \cdot w}$, i.e., thermal conductivity of the fin does not appear in the expression for the temperature distribution. This is to be expected since diffusion is assumed to be negligible in this special case.

5.1.2. Negligible advection

The other extreme scenario of theoretical interest is where advection is small or negligible. In such a case, the second term on the left hand of the governing energy equation may be neglected. This results in

$$\frac{1}{\xi}\frac{\partial}{\partial\xi}\left(\xi\frac{\partial\theta}{\partial\xi}\right) - \bar{B}\theta = 0 \tag{22}$$

which is indeed the standard governing equation for a purely diffusive fin. A general solution for this problem obtained by setting $\bar{A} = 0$ in the general solution, Eq. (10) is

$$\theta(\xi) = c_1 I_0\left(\sqrt{\bar{B}}\xi\right) + c_2 K_0\left(\sqrt{\bar{B}}\xi\right) \tag{23}$$

which matches with the standard solution for this pure-diffusive problem [1]. The constants appearing in Eq. (23) may be obtained using boundary conditions, similar to the general case considered in Section 2. For example, for an adiabatic tip, one may derive

$$\theta(\xi) = \frac{K_1\left(\sqrt{\bar{B}}(1+\bar{L})\right)I_0\left(\sqrt{\bar{B}}\xi\right) + I_1\left(\sqrt{\bar{B}}(1+\bar{L})\right)K_0\left(\sqrt{\bar{B}}\xi\right)}{K_1\left(\sqrt{\bar{B}}(1+\bar{L})\right)I_0\left(\sqrt{\bar{B}}\right) + I_1\left(\sqrt{\bar{B}}(1+\bar{L})\right)K_0\left(\sqrt{\bar{B}}\right)} \tag{24}$$

5.2. Tip boundary special cases

While the model presented in Section 2 assumes general convective boundary conditions at the tip, including a general tip ambient temperature, depending on the specific conditions encountered in a problem, a number of simplifications may be considered.

A commonly encountered special case is that of an adiabatic tip. This may be relevant, for example, when heat transfer at the tip may be negligible due to the small tip area, or because the fin is very long. In either case, temperature distribution in the fin may be obtained by setting $Bi_{tip} = 0$ in Eqs. (10), (13) and (14), resulting in

$$\theta(\xi) = \xi^{\bar{A}/2}\frac{K_{\frac{\bar{A}}{2}-1}\left(\sqrt{\bar{B}}(1+\bar{L})\right)I_{\bar{A}/2}\left(\sqrt{\bar{B}}\xi\right) + I_{\frac{\bar{A}}{2}-1}\left(\sqrt{\bar{B}}(1+\bar{L})\right)K_{\bar{A}/2}\left(\sqrt{\bar{B}}\xi\right)}{K_{\frac{\bar{A}}{2}-1}\left(\sqrt{\bar{B}}(1+\bar{L})\right)I_{\frac{\bar{A}}{2}}\left(\sqrt{\bar{B}}\right) + I_{\frac{\bar{A}}{2}-1}\left(\sqrt{\bar{B}}(1+\bar{L})\right)K_{\frac{\bar{A}}{2}}\left(\sqrt{\bar{B}}\right)} \tag{25}$$

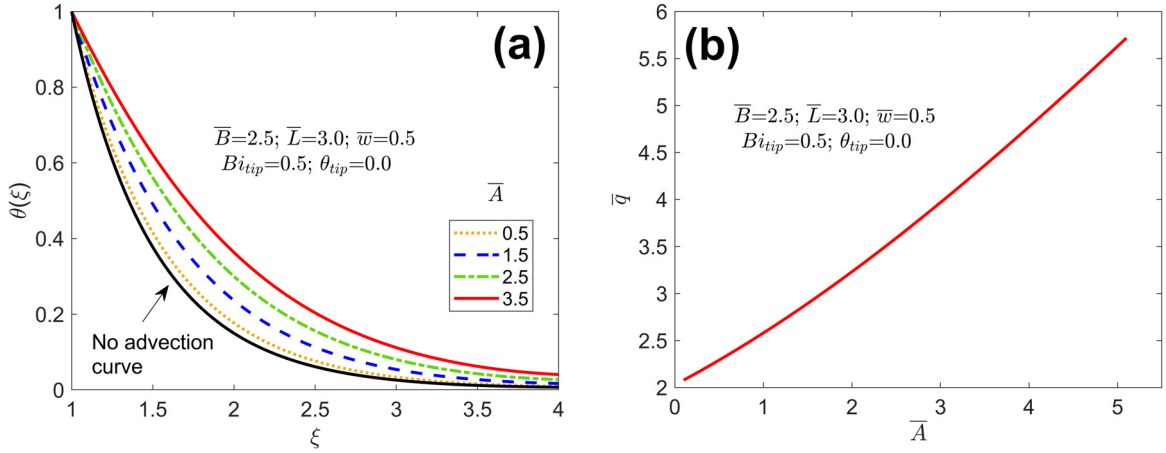

Fig. 3. Impact of $\bar{A}$: (a) fin temperature distribution for multiple values of $\bar{A}$, (b) heat transfer rate $\bar{q}$ as a function of $\bar{A}$. Other problem parameters are $\bar{B} = 2.5$, $\bar{L} = 3.0$, $\bar{w} = 0.5$, $Bi_{tip} = 0.5$ and $\theta_{\infty,tip} = 0.0$.

While the adiabatic tip excludes any heat transfer at the tip, the opposite, best-case scenario for heat transfer at the tip arises when the tip is specified to be at a certain temperature $\theta_{\infty,tip}$. Results for this case may be obtained by setting $Bi_{tip} \to \infty$ in Eqs. (10), (13) and (14), which results in

$$\theta(\xi) = \xi^{\bar{A}/2} \frac{\left(K_{\frac{\bar{A}}{2}}\left(\sqrt{\bar{B}}(1+\bar{L})\right) - \theta_{\infty,tip}K_{\frac{\bar{A}}{2}}\left(\sqrt{\bar{B}}\right)\right)I_{\bar{A}/2}\left(\sqrt{\bar{B}}\xi\right) - \left(I_{\frac{\bar{A}}{2}}\left(\sqrt{\bar{B}}(1+\bar{L})\right) - \theta_{\infty,tip}I_{\frac{\bar{A}}{2}}\left(\sqrt{\bar{B}}\right)\right)I_{\bar{A}/2}\left(\sqrt{\bar{B}}\xi\right)}{K_{\frac{\bar{A}}{2}}\left(\sqrt{\bar{B}}(1+\bar{L})\right)I_{\frac{\bar{A}}{2}}\left(\sqrt{\bar{B}}\right) - I_{\frac{\bar{A}}{2}}\left(\sqrt{\bar{B}}(1+\bar{L})\right)K_{\frac{\bar{A}}{2}}\left(\sqrt{\bar{B}}\right)} \tag{26}$$

Finally, in many scenarios, the freestream temperature associated with the convective boundary condition at the tip is the same as the ambient temperature, i.e., $\theta_{\infty,tip} = 0$. In such a case, temperature distribution in the fin further simplifies to

$$\theta(\xi) = \xi^{\bar{A}/2} \frac{K_{\frac{\bar{A}}{2}}\left(\sqrt{\bar{B}}(1+\bar{L})\right)I_{\bar{A}/2}\left(\sqrt{\bar{B}}\xi\right) - I_{\frac{\bar{A}}{2}}\left(\sqrt{\bar{B}}(1+\bar{L})\right)I_{\bar{A}/2}\left(\sqrt{\bar{B}}\xi\right)}{K_{\frac{\bar{A}}{2}}\left(\sqrt{\bar{B}}(1+\bar{L})\right)I_{\frac{\bar{A}}{2}}\left(\sqrt{\bar{B}}\right) - I_{\frac{\bar{A}}{2}}\left(\sqrt{\bar{B}}(1+\bar{L})\right)K_{\frac{\bar{A}}{2}}\left(\sqrt{\bar{B}}\right)} \tag{27}$$

Expressions for fin performance parameters, including heat removal rate, fin effectiveness and porous fin effectiveness can be simplified similarly.

6. Results and Discussion

6.1. Impact of $\bar{A}$ and $\bar{B}$ on fin temperature distribution

$\bar{A}$ and $\bar{B}$ are the two key non-dimensional parameters that appear in the governing energy equation, and consequently in the expressions for temperature distribution and fin performance parameters. $\bar{A}$ represents heat advection due to the radial porous flow in the fin driven by the imposed pressure gradient, relative to diffusive heat flow, and thus, is a Péclet number. On the other hand, $\bar{B}$ represents the rate of heat loss from the fin surface to the surrounding, also relative to diffusive heat flow, and is similar to the Damköhler number in mass transfer analysis. It is pertinent to examine the impact of these key non-dimensional parameters on the fin temperature distribution and fin performance.

Fig. 3 examines the impact of $\bar{A}$. A number of temperature distribution curves for different values of $\bar{A}$ are plotted in Fig. 3(a). The values of other parameters are $\bar{B} = 2.5$, $\bar{L} = 3.0$, $\bar{w} = 0.5$, $\theta_{\infty,tip} = 0.0$ and $Bi_{tip} = 0.5$. For comparison, the zero advection curve corresponding to a non-porous fin is also plotted. Fig. 3(a) shows that the fin temperature curves shift upwards with increasing value of $\bar{A}$, which can be attributed to greater heat removal down the fin at large $\bar{A}$ due to advection, which increases the fin temperature in general. The curves for various values of $\bar{A}$ approach the limiting case of the traditional non-porous fin as $\bar{A}$ decreases. Note that in each case, as expected, the temperature at the fin base ($\xi = 1$) has a value of 1, whereas the magnitude and gradient of the temperature distribution at the fin tip, $\xi = 1 + \bar{L}$, is determined by the convective boundary condition at the tip.

The impact of $\bar{A}$ on fin performance is further shown in Fig. 3(b), in which the total heat removed by the fin, given by Eq. (17), is plotted as a function of $\bar{A}$. Even though conductive heat removal decreases with increasing $\bar{A}$, as evidenced by the decreasing slope of temperature plots at the base seen in Fig. 3(a), yet, the increased advective heat transfer at large $\bar{A}$ results in increasing total heat removed with increasing $\bar{A}$.

Note that several dimensional parameters and properties contribute towards $\bar{A}$, as defined in Eq. (5). For example, increasing the permeability or pressure gradient, reducing the viscosity or reducing the fin length relative to its radius all contribute towards increasing $\bar{A}$, and thus improving fin performance. Note that the fin porosity impacts fin performance in a more complicated manner, because while $\bar{A}$ increases with increasing fin porosity, it also reduces the effective thermal conductivity k_{eff}, thereby affecting other non-dimensional parameters such as $\bar{B}$ too. This is examined in more detail in a later sub-section.

In contrast with $\bar{A}$, which represents advective cooling, $\bar{B}$ represents heat removal due to convective heat transfer from the fin surface to the surrounding ambient. The impact of $\bar{B}$ on fin temperature distribution and heat removal is investigated in Fig. 4. Fin temperature curves for multiple values of $\bar{B}$ are plotted in Fig. 4(a), whereas total heat removal is plotted as a function of $\bar{B}$ in Fig. 4(b). All other problem parameters are the same as Fig. 3, along with $\bar{A} = 2.5$. As expected, the larger the value of $\bar{B}$, the greater is the heat removed from the fin, and, therefore, the cooler is the fin. Fig. 4(a) also shows strong dependence of the slope of the temperature curve at the fin base on $\bar{B}$, which indicates greater heat removal from the base as $\bar{B}$ increases. This is also seen more directly

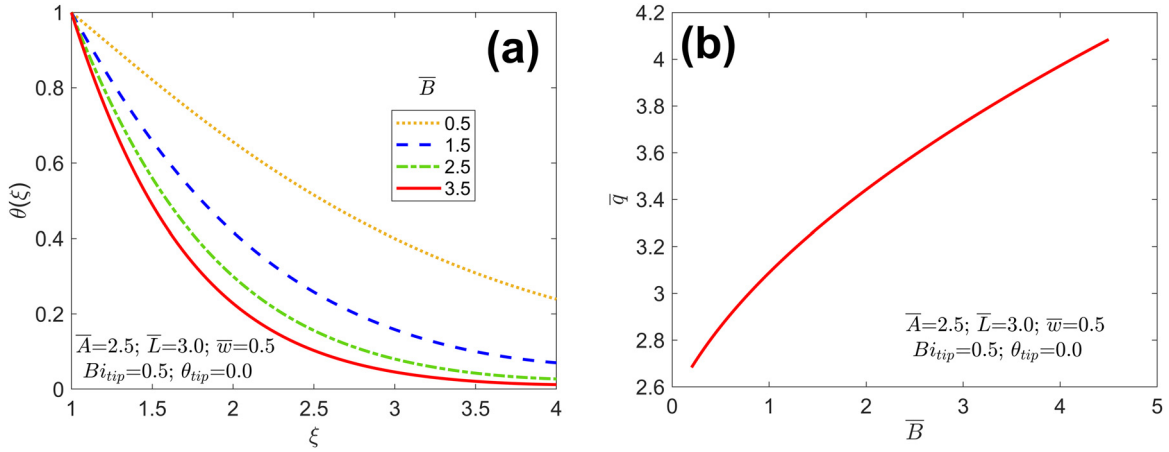

Fig. 4. Impact of $\bar{B}$: (a) fin temperature distribution for multiple values of $\bar{B}$, (b) heat transfer rate $\bar{q}$ as a function of $\bar{B}$. Other problem parameters are $\bar{A} = 2.5$, $\bar{L} = 3.0$, $\bar{w} = 0.5$, $Bi_{tip} = 0.5$ and $\theta_{\infty,tip} = 0.0$.

in the heat removal plot in Fig. 4(b), where the heat removed by the fin is seen to increase with increasing value of $\bar{B}$.

Per Eq. (5), the key physical quantity that appears in the expression for $\bar{B}$ is the convective heat transfer coefficient around the fin, h. All other parameters being the same, the greater the value of h, the greater is the heat removal to surroundings. This is clearly seen in Figs. 4(a) and 4(b). Note that while several other dimensional parameters also appear in the expression for $\bar{B}$, most notably the effective thermal conductivity (as well as the porosity that appears within k_{eff}), these parameters also influence other non-dimensional numbers. Therefore, the influence of these parameters is analyzed separately in a later sub-section.

6.2. Fin Performance Parameters

Section 4 defines two key performance parameters of the fin. These parameters represent how much heat is removed by the porous fin relative to the no fin case, and relative to a comparable non-porous fin. The impact of key non-dimensional numbers appearing in the problem – $\bar{A}$ and $\bar{B}$ – on these two parameters is investigated in detail.

6.2.1. Fin Effectiveness, η

The fin effectiveness, η is considered first. As defined in Eq. (18), η represents heat removal by the porous fin relative to the baseline case without any fin at all. Fig. 5 plots η as the function of the non-dimensional convective heat transfer coefficient $\bar{B}$. Curves are presented for multiple values of $\bar{A}$. In each case, fin effectiveness reduces with increasing $\bar{B}$, rapidly at first, followed by a plateau at larger values of $\bar{B}$. Also, the curves in Fig. 5 shift upwards with increasing value of $\bar{A}$. This is because at large $\bar{B}$, there is relatively large convective heat removal, implying that the performance of the fin is increasingly closer to heat removal without the fin at all. In contrast, $\bar{A}$ simply appears as an additional term in the fin effectiveness expression given in Eq. (18), and, therefore simply shifts the curves upwards.

The impact of $\bar{B}$ is also confirmed from Fig. 4(a) that shows that the magnitude of the slope of the temperature curve at $\xi = 1$ increases with $\bar{B}$, but does not change appreciably at large $\bar{B}$. This explains the plateauing out of the curves in Fig. 5.

These results indicate that when the non-dimensional convective heat transfer coefficient is relatively large, increasing the advective heat removal, for example, by making the fin more porous does not significantly improve fin performance. This is because the rate-limiting step is the conductive heat removal from the fin. The impact of porosity on performance of the porous fin is likely to be

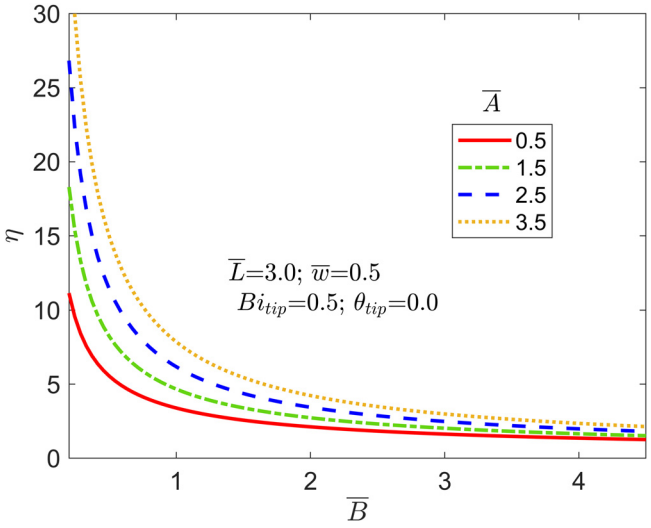

Fig. 5. Fin effectiveness as a function of $\bar{B}$ for multiple values of $\bar{A}$. Other problem parameters are $\bar{L} = 3.0$, $\bar{w} = 0.5$, $Bi_{tip} = 0.5$ and $\theta_{\infty,tip} = 0.0$.

significant when the convective heat removal from the fin surface is not very strong, for example, in conditions approaching natural convection around the fin.

The fin effectiveness plotted in Fig. 5 is found to be greater than one throughout the parameter space considered here, indicating that more heat is removed by the fin than without, which is desirable. It is found that the fin effectiveness flattens out at large values of $\bar{B}$. This is because when the convective heat transfer coefficient around the fin is very large, then the effect of increased surface area due to the fin is not very significant any more.

In contrast with Fig. 5, fin effectiveness is plotted as a function of $\bar{A}$ in Fig. 6. As expected, fin effectiveness increases monotonically with $\bar{A}$, which is because $\bar{A}$ appears as an independent term in the expression of η, given by Eq. (18). As expected, the larger the value of $\bar{B}$, the lower are the effectiveness curves in Fig. 6. This is mainly because, as shown and discussed in Fig. 5, fin effectiveness reduces with increasing $\bar{B}$.

6.2.2. Porous Fin Effectiveness, η_{porous}

The porous fin effectiveness η_{porous} which compares performance of the porous fin with that of a comparable non-porous fin is considered next. Similar to Figures in the previous sub-section, η_{porous} is plotted as a function of $\bar{B}$ for multiple values of $\bar{A}$ in

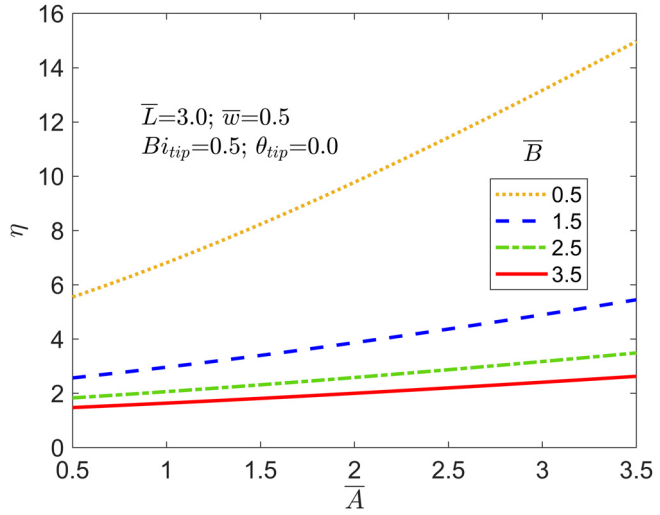

Fig. 6. Fin effectiveness as a function of $\bar{A}$ for multiple values of $\bar{B}$. Other problem parameters are $\bar{L} = 3.0$, $\bar{w} = 0.5$, $Bi_{tip} = 0.5$ and $\theta_{\infty,tip} = 0.0$.

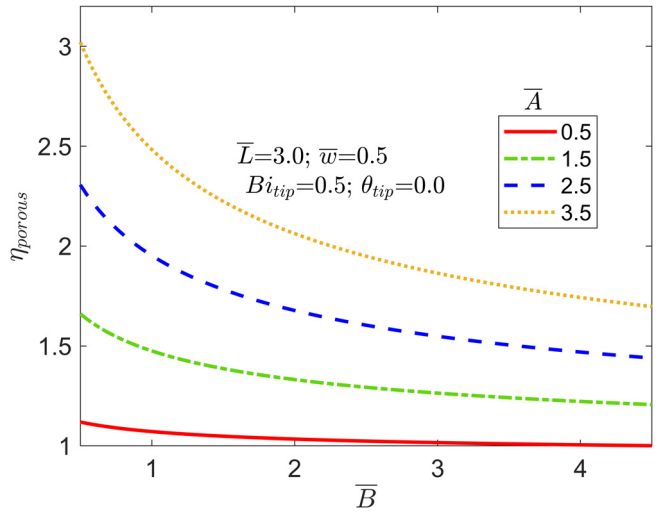

Fig. 7. Porous fin effectiveness as a function of $\bar{B}$ for multiple values of $\bar{A}$. Other problem parameters are $\bar{L} = 3.0$, $\bar{w} = 0.5$, $Bi_{tip} = 0.5$ and $\theta_{\infty,tip} = 0.0$.

Fig. 7, and as a function of $\bar{A}$ for multiple values of $\bar{B}$ in Fig. 8. These curves show strong dependence of η_{porous} on $\bar{A}$, and relatively weaker dependence on $\bar{B}$, particularly at small $\bar{A}$. This is mainly because the key difference between the porous fin and the non-porous fin is the porous convective term $\bar{A}$. The greater the value of $\bar{A}$, the greater is the heat removal by the porous fin compared to the non-porous fin, which is completely unaffected by $\bar{A}$. This can also be confirmed mathematically from the expression of $\bar{q}$, given by Eq. (17). Therefore, the porous fin becomes more and more attractive compared to the non-porous fin as $\bar{A}$ increases.

In contrast, the porous fin effectiveness is not as strongly dependent on $\bar{B}$, particularly for small values of $\bar{A}$. This is because when $\bar{A}$ is small, there is no particular distinction between the porous and non-porous fin, and no particular thermal advantage of the porous fin over the non-porous fin. Since $\bar{B}$ is expected to affect both porous and non-porous fins similarly, therefore, when $\bar{A}$ is small, the fin performance is not significantly impacted by $\bar{B}$, and η_{porous} is close to one, indicating that the porous and non-porous fins have nearly the same performance.

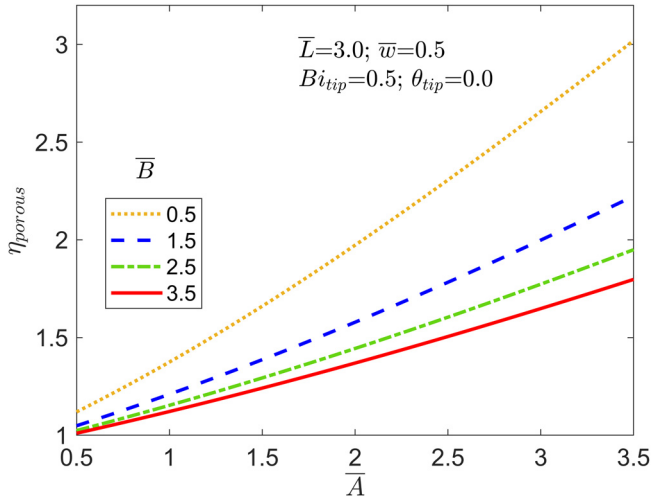

Fig. 8. Porous fin effectiveness as a function of $\bar{A}$ for multiple values of $\bar{B}$. Other problem parameters are $\bar{L} = 3.0$, $\bar{w} = 0.5$, $Bi_{tip} = 0.5$ and $\theta_{\infty,tip} = 0.0$.

6.3. Effect of porosity: Trade-off between conductive and advective heat removal

The parallel placement of R_{cond} and R_{adv} in the resistance network shown in Fig. 2 presents interesting trade-offs and opportunities for optimization of fin performance. Specifically, it is of interest to examine how these two components change as the porosity of the fin is changed since changing the porosity of the fin material is an important design question. In general, increasing the porosity is expected to reduce the effective thermal conductivity, per Eq. (15), since the solid material comprising the fin is likely to have greater thermal conductivity than the fluid. This is expected to lead to reduced conductive heat removed by the fin. On the other hand, greater porosity also results in greater area available for porous fluid flow, and, thus, greater advective heat removal. Mathematically, this can be seen in the $\bar{A}$ term that increases with increasing porosity due to the ϕ and k_{eff} terms in the numerator and denominator, respectively, and that results in greater fin heat removal, per Eq. (5). Moreover, the porosity ϕ appearing in the advection term in the energy conservation equation given by Eq. (1) also shows the enhancement in advective heat removal due to increased porosity. The opposing effects of porosity on conductive and advective heat removal pose an interesting theoretical question about whether an optimal porosity exists that maximizes or minimizes total heat removal. This is also a question of much practical relevance, and, therefore, is investigated in more detail.

To begin with, heat removed by a representative porous fin is considered. The baseline solid material is assumed to be aluminum, and the fluid is assumed to be air, with constant properties corresponding to room temperature. Permeability of the fin is taken to be K=5.7 $\times$ 10^{-9} m^2. The inner radius fin length and fin width are taken to be R_0=5 cm, L=15 cm and w=5 cm, respectively. The pressure difference driving the porous flow is taken to be $\Delta p = 100$ Pa. The convective heat transfer coefficient, both around the fin and at the tip is taken to be h_{tip}=50 Wm^{-2}K^{-1}. Under these conditions, Fig. 9 presents the total heat removed as well as the conductive and advective components as functions of porosity, corresponding to 20°C temperature difference between the base and ambient. As expected from the discussion above, the conductive and advective components of heat removed decrease and increase, respectively, with increasing porosity. While the advective component increases nearly linearly, the advective component has a more complicated, non-linear reduction. This is because aside from the effect on effective thermal conductivity, porosity in-

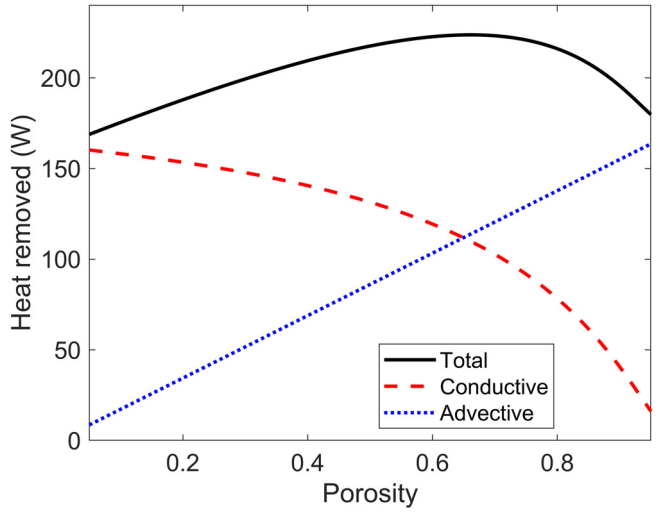

Fig. 9. Heat removal rate as a function of fin porosity for a baseline set of design parameters. Total heat removed as well as the conductive and advective components are plotted.

creases the advective term in the governing energy equation ($\bar{A}$) linearly, whereas the impact of porosity on conductive heat transfer is more complicated, driven by the slope of the temperature distribution at the base, as given by the solution involving modified Bessel functions. Interestingly, in this case, the total heat removed changes non-monotonically with porosity and exhibits a maxima at a porosity of around 0.65. This shows the importance of careful design of the porous fin, particularly its porosity in order to maximize the benefit of the porous fin.

Note that the impact of porosity on fin effectiveness is somewhat complicated due to the number of ways in which the porosity affects heat removal rate, depending on the values of various problem parameters and non-dimensional numbers that appear in the analysis presented above. While an optimal porosity is found for the set of parameters considered above, the location of the optimal porosity, or even the existence of an optimal porosity itself is not universal. For example, the impact of the convective heat transfer on these curves is examined. Figs. 10(a) and 10(b) plot the total heat removed as well as the conductive and advective components as functions of porosity for h=12 $Wm^{-2}K^{-1}$ and h=150 $Wm^{-2}K^{-1}$, respectively. All other parameters remain the same. It is found that changing the convective heat transfer coefficient completely changes the nature of the heat removal curves. The non-monotonic behavior of total heat removed seen in Fig. 9 is not seen any longer in Figs. 10(a) and 10(b). It is found instead that the total heat removed increases (Fig. 10(a)) or decreases (Fig. 10(b)) monotonically with porosity when the convective heat transfer coefficient is lower or higher, respectively, than the value considered in Fig. 9. This is mainly because increasing h reduces the convective resistance at the fin surface, R_{surf}, as shown in Fig. 2 without impacting the advective resistance R_{adv}. As a result, more heat is drawn conductively through while the advective component remains the same. As a result, the total heat removed is dominated by the conductive component, and, thus shows a decreasing trend with porosity, as seen in Fig. 10(b). A similar explanation may be provided for the impact of reducing h on heat removal rates.

Fig. 10 shows that when the convective heat transfer is very small, such as in natural convection conditions around the fin, it is best to design the fin to be as porous as possible, within other constraints such as structural integrity. On the other hand, as shown in Fig. 10(b), under forced convective conditions around the fin, having a porous fin is not beneficial at all, since the improvement in advective heat removal with increasing porosity is completely overwhelmed by the reduction in conductive heat removal as porosity increases.

As another illustration of the impact of design parameters on how the heat removal rate varies with porosity, the same baseline case as Fig. 9 is considered again, but with different values of the imposed pressure gradient. In contrast with the baseline value of $\Delta p = 100$ Pa, Figs. 11(a) and 11(b) plot heat removal curves as functions of porosity for $\Delta p = 400$ Pa and $\Delta p = 20$ Pa, respectively. It is found that while a greater pressure difference results in a monotonically increasing heat removal rate as a function of porosity, a lower pressure difference completely reverses the trend, resulting in a monotonically decreasing heat removal rate as a function of porosity. This is mainly because changing the pressure difference affects the advective resistance R_{adv} without affecting any other resistances in the problem, thereby making the total heat removal more dominant or less dominant by advective or conductive heat removal, respectively, at larger or smaller pressure differences.

Similar to the effect of the convective heat transfer coefficient examined in Fig. 10, this analysis shows that determining whether a porous fin is beneficial or not and, if so, selecting the best porosity depends strongly on the available pressure difference that drives the porous flow. For very large pressure difference, the larger the porosity, the more effective is the fin. In contrast, for very small pressure difference, there may be little or no benefit of using a porous fin.

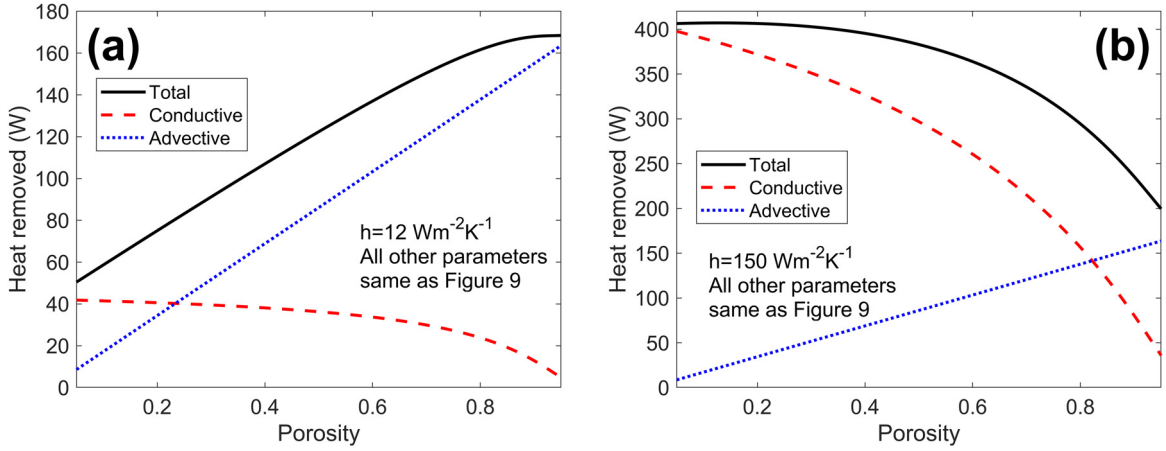

Fig. 10. Heat removal rate as a function of fin porosity for (a) h = 10 $Wm^{-2}K^{-1}$ and (b) h = 150 $Wm^{-2}K^{-1}$. Other parameters are the same as Fig. 9. Total heat removed as well as the conductive and advective components are plotted.

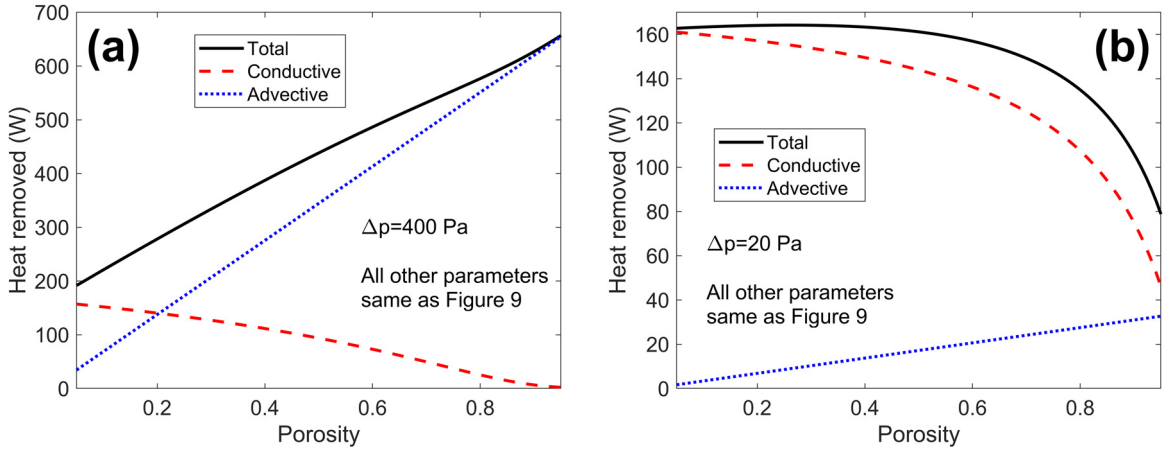

Fig. 11. Heat removal rate as a function of fin porosity for (a) $\Delta p = 400$ Wm^{-2}K^{-1} and (b) $\Delta p = 20$ Wm^{-2}K^{-1}. Other parameters are the same as Fig. 9. Total heat removed as well as the conductive and advective components are plotted.

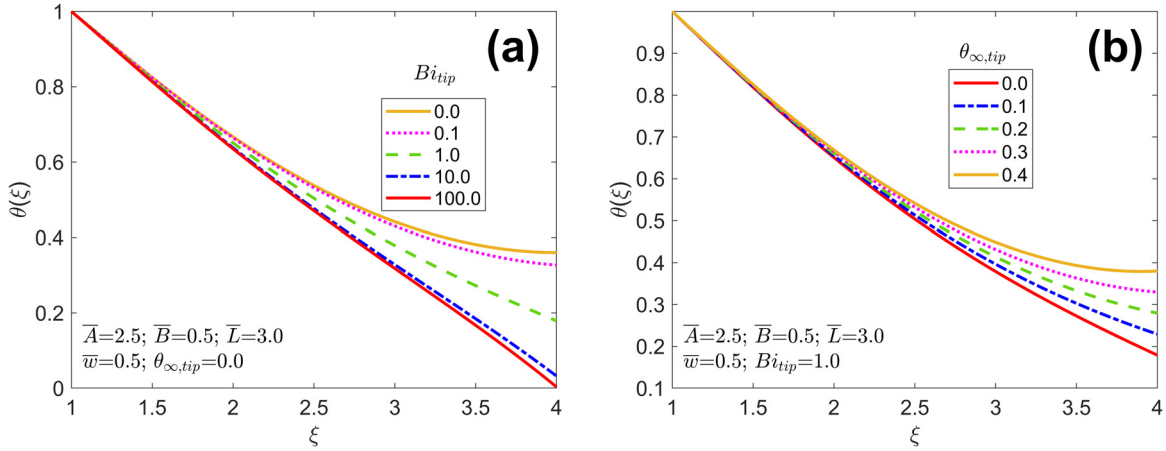

Fig. 12. Effect of fin tip conditions: Fin temperature distribution for (a) multiple values of Bi_{tip}, with $\theta_{\infty,tip} = 0.0$, (b) multiple values of $\theta_{\infty,tip}$ with $Bi_{tip} = 1.0$. Other problem parameters are $\bar{A} = 2.5$, $\bar{B} = 0.5$, $\bar{L} = 3.0$ and $\bar{w} = 0.5$.

Whether an optimal value of the porosity exists, and if so, determining that value can be addressed by examining the derivative of the total heat removed with respect to the porosity. Differentiating Eq. (16) and setting to zero results in

$$\left(k_f - k_s\right)\left(\frac{\partial\theta}{\partial\xi}\right)_{\xi=1} + k_{eff}\frac{\partial}{\partial\phi}\left[\left(\frac{\partial\theta}{\partial\xi}\right)_{\xi=1}\right] - \frac{\mathrm{K}\cdot\rho_f c_f\cdot\Delta p}{\mu\cdot\ln\left(\frac{R_0+L}{R_0}\right)} = 0 \tag{28}$$

The root of Eq. (28), if one exists between 0 and 1 is the optimal porosity for maximizing heat removal by the fin.

6.4. Effect of tip conditions

Similar to a traditional, non-porous fin, the nature of the convective boundary conditions at the fin tip is expected to influence the temperature distribution in the porous fin. The two key non-dimensional parameters that describe thermal conditions at the fin tip are the tip Biot number Bi_{tip} and tip temperature $\theta_{\infty,tip}$. As discussed in Section 3, specific values of these parameters transform the general problem considered here into special cases, such as an adiabatic tip or an isothermal tip.

In order to examine the impact of Bi_{tip} and $\theta_{\infty,tip}$ on thermal response of the fin, the fin temperature distribution is plotted for multiple values of Bi_{tip} and $\theta_{\infty,tip}$ in Figs. 12(a) and 12(b), respectively. Fig. 12(a) is plotted for $\theta_{\infty,tip} = 0.0$, while Fig. 12(b) is plotted for $Bi_{tip} = 1.0$. Other non-dimensional parameters are $\bar{A} = 2.5$, $\bar{B} = 0.5$, $\bar{L} = 3.0$ and $\bar{w} = 0.5$. Fig. 12(a) shows that for $Bi_{tip} = 0.0$, the fin is, in general, the hottest. This, however, does not imply greater heat removal, since all curves in Fig. 12(a) have nearly the same slope at $\xi = 1$. Note that $Bi_{tip} = 0.0$ renders the fin tip adiabatic, resulting in no heat removal from the end of the fin, as confirmed by the flat nature of the $Bi_{tip} = 0.0$ curve at $\xi = \bar{L}$. As Bi_{tip} increases, the fin temperature curves shift downwards and the slope at the fin tip becomes larger in magnitude, indicating increased heat loss from the fin tip. However, the effect of fin tip conditions does not extend throughout the fin, and, in particular, significantly does not influence heat removal from the base. For very large value of Bi_{tip}, Fig. 12(a) shows that the fin tip temperature becomes very close to $\theta_{\infty,tip}$, approaching isothermal fin tip conditions. Note that the tip temperature for both $Bi_{tip} = 10.0$ and $Bi_{tip} = 100.0$ curves is close to $\theta_{\infty,tip}$, indicating that both values of the Biot number are close to isothermal conditions.

The impact of $\theta_{\infty,tip}$ is examined in Fig. 12(b). In this case, $Bi_{tip} = 1.0$, which is a reasonably low value. This is the reason why the temperature curves in Fig. 12(b) do not reach $\theta_{\infty,tip}$ at the tip. Nevertheless, the lower the value of $\theta_{\infty,tip}$, the lower is the temperature curve in general. Note that for relatively large value of $\theta_{\infty,tip} = 0.4$, the temperature curve actually reaches a minima within the fin and then rises towards the fin tip, indicating that

some parts of the fin may be cooler than the fin tip. This only occurs for large value of $\theta_{\infty,tip}$, which is likely unrealistic, since the fin tip is unlikely to be hotter than the ambient around the fin. In most cases, the two are expected to be the same, and, therefore, $\theta_{\infty,tip} = 0.0$ is the most likely scenario.

Note that in both Figs. 12(a) and 12(b), changing the tip conditions, i.e., Bi_{tip} and $\theta_{\infty,tip}$, does not appreciably change the slope of the temperature at the base of the fin. This indicates that the conductive heat removed by the fin is largely independent of the tip conditions. Since the convective heat removal also does not depend on Bi_{tip} and $\theta_{\infty,tip}$, therefore, under the conditions considered here, fin performance is largely independent of the fin tip. This may be because of the relatively large length of the fin considered here. For a shorter fin, it is likely that increasing the tip Biot number may have a stronger impact on the non-dimensional fin heat removal.

7. Conclusions

The key contributions of this work include the thermal analysis of a radial porous fin in which heat removal is aided by radial pressure-driven flow instead of natural convection flow considered in past papers, and the identification of key conduction-vs-advection trade-offs in fin design. Under a certain set of parameters, it is shown that there exists a fin porosity that maximizes heat removal rate. Under certain other set of parameters, it is shown that a porous fin may not offer any benefits at all over a non-porous fin of the same geometry. These insights may be helpful to choosing whether to use a porous fin or not in a given heat transfer problem, and if so, the correct porosity to choose.

Non-dimensional curves presented in this work improve the general understanding of extended surface heat transfer, particularly in the context of porous fins. Such curves may be useful for the general design of heat transfer systems.

It must be noted that this work analyzes only the heat transfer aspects of a porous fin. A highly porous fin is also light-weight. Weight reduction may be desirable for certain applications, but it comes at the cost of reduced ability to withstand mechanical loads. For applications where weight and load bearing capability are important, such mechanical considerations must also be accounted for in fin design and optimization, in addition to the thermal analysis presented here. In addition, the pumping power needed to sustain the pressure-driven flow, which is not considered here, may be important in certain problems.

While the porous flow in this work is assumed to be driven by a pressure gradient, other fluid flow mechanisms, such as electro-osmotic flow can be easily analyzed within the same framework as the one presented here. The present work assumes negligible natural convection of the porous fluid within the fin. Radiative effects have also been neglected due to a reasonably small temperature difference. Thermal properties of the fin material and fluid are assumed to be independent of temperature. Porous fluid flow is assumed to be Newtonian and laminar, and with constant permeability. While these assumptions are reasonable for a wide range of applications, in other problems, several of these assumptions can potentially be relaxed, in which case, the use of numerical techniques to solve the resulting equations may be necessary. Nevertheless, several important trade-offs identified here may persist even in such scenarios.

Declaration of Competing Interest

The authors declare that they have no known competing financial interests or personal relationships that could have appeared to influence the work reported in this paper.

CRediT authorship contribution statement

Ankur Jain: Conceptualization, Methodology, Formal analysis, Validation, Investigation, Data curation, Project administration, Writing – original draft, Writing – review & editing. **Muhammad M. Abbas:** Formal analysis, Validation, Data curation. **Mohsen Torabi:** Conceptualization, Methodology, Writing – original draft, Writing – review & editing.

Data availability

Data will be made available on request.

Appendix A. Derivation of radial velocity field in the porous fin

This Appendix derives an expression for the velocity field in the porous fin. Based on the assumptions listed in Section 2, fluid flow in the fin is driven by the pressure gradient between the inner pipe and the ambient at the fin tip, and is purely radial in nature. Assuming that the porous fluid flow is purely Darcian in nature, the following relationship exists between the volumetric flow rate q and local pressure gradient at any location r [9,10]:

$$q = \frac{KA}{\mu}\frac{dp}{dr} \tag{A.1}$$

Where $A = 2\pi rw\phi$ is the cross-section area for fluid flow at the radial location r, and K, ϕ, and μ are the permeability, porosity and viscosity, respectively. Rearranging and integrating equation (A.1) between $r = R_0$ and $r = R_0 + L$ results in

$$q = \frac{KA}{\mu \cdot \ln\left(\frac{R_0+L}{R_0}\right)}\frac{\Delta p}{r} \tag{A.2}$$

Where Δp is the total pressure difference between the inner tube and the fin tip. Finally, since $q = A \cdot U(r)$, therefore, the following expression for the velocity field may be written:

$$U(r) = \frac{K}{\mu \cdot \ln\left(\frac{R_0+L}{R_0}\right)}\frac{\Delta p}{r} \tag{A.3}$$

This completes the derivation of the radial velocity field in the porous fin. As expected, the radial velocity has a $1/r$ dependence, due to the requirement of mass conservation as the fluid flows radially outwards.

References

[1] A.D. Kraus, A.M. Aziz, J.R. Welty, Extended Surface Heat Transfer, John Wiley, New York, 2002.
[2] R.L. Webb, B. Sunden, N.-H. Kim, Principles of Enhanced Heat Transfer, Routledge, Boca Raton, 2005.
[3] R.J. McGlen, R. Jachuck, S. Lin, Integrated thermal management techniques for high power electronic devices, Appl. Therm. Eng. 24 (2004) 1143–1156, doi:10.1016/j.applthermaleng.2003.12.029.
[4] A. Mostafavi, M. Parhizi, A. Jain, Theoretical modeling and optimization of fin-based enhancement of heat transfer into a phase change material, Int. J. Heat Mass Transf. 145 (2019) 118698 1-10, doi:10.1016/j.ijheatmasstransfer.2019.118698.
[5] H.H. Pennes, Analysis of tissue and arterial blood temperatures in the resting human forearm, J. Appl. Physiol. 1 (1948) 93–122, doi:10.1152/jappl.1948.1.2.93.
[6] S.-H. Park, J.H. Jeong, Analytical fin efficiency model for open-cell porous metal fins based on Kelvin cell assumption, Int. J. Heat Mass Transf. 196 (2022) 123283, doi:10.1016/j.ijheatmasstransfer.2022.123283.
[7] S. Kiwan, M.A. Al-Nimr, Using porous fins for heat transfer enhancement, ASME J. Heat Mass Transf. 123 (4) (2001) 790–795, doi:10.1115/1.1371922.
[8] M. Torabi, H. Yaghoobi, Series solution for convective-radiative porous fin using differential transformation method, J. Porous Media 16 (2013) 341–349, doi:10.1615/JPorMedia.v16.i4.60.
[9] D.A. Nield, A. Bejan, Convection in Porous Media, 4th Ed., Springer, 2013.
[10] M. Kaviany, Principles of Heat Transfer in Porous Media, 2nd Ed., Springer New York, NY, 1995, doi:10.1007/978-1-4612-4254-3.
[11] F.M. White, Viscous Fluid Flow, 3rd Ed., McGraw Hill, 2005.

[12] S. Saedodin, M. Shahbabaaei, Thermal analysis of natural convection in porous fins with homotopy perturbation method (HPM), Arab. J. Sci. Eng. 38 (2013) 2227–2231, doi:10.1007/s13369-013-0581-6.
[13] T. Zhao, H. Tian, L. Shi, T. Chen, X. Ma, M. Atik, G. Shu, Numerical analysis of flow characteristics and heat transfer of high-temperature exhaust gas through porous fins, Appl. Therm. Eng. 165 (2020) 114612, doi:10.1016/j.applthermaleng.2019.114612.
[14] H. Kahalerras, N. Targui, Numerical analysis of heat transfer enhancement in a double pipe heat exchanger with porous fins, Int. J. Numer. Methods for Heat & Fluid Flow 18 (2008) 593–617, doi:10.1108/09615530810879738 2008.
[15] S. Kiwan, Thermal analysis of natural convection porous fins, Transp Porous Media 67 (2007) 17–29, doi:10.1007/s11242-006-0010-3.
[16] R. Das, Forward and inverse solutions of a conductive, convective and radiative cylindrical porous fin, Energy Conv. Management 87 (2014) 96–106, doi:10.1016/j.enconman.2014.06.096.
[17] M. Hatami, D.D. Ganji, Thermal performance of circular convective–radiative porous fins with different section shapes and materials, Energy Conv. Management 76 (2013) 185–193, doi:10.1016/j.enconman.2013.07.040.
[18] M. Turkyilmazoglu, Efficiency of heat and mass transfer in fully wet porous fins: exponential fins versus straight fins, Int. J. Refrig. 46 (2014) 158–164, doi:10.1016/j.ijrefrig.2014.04.011.
[19] D.S. Kumar, S. Jayavel, Optimization of porous fin location and investigation of porosity and permeability effects on hydro-thermal behavior of rectangular microchannel heat sink, Int. Communic. Heat Mass Transf. 129 (2011) 105737, doi:10.1016/j.icheatmasstransfer.2021.105737.
[20] B. Kundu, D. Bhanja, K.-S. Lee, A model on the basis of analytics for computing maximum heat transfer in porous fins, Int. J. Refrig. 55 (2012) 7611–7622, doi:10.1016/j.ijheatmasstransfer.2012.07.069.
[21] M. Hatami, A. Hasanpour, D.D. Ganji, Heat transfer study through porous fins (Si_3N_4 and Al) with temperature-dependent heat generation, Energy Conv. Management 74 (2013) 9–16, doi:10.1016/j.enconman.2013.04.034.
[22] J. Ma, Y. Sun, B. Li, H. Chen, Spectral collocation method for radiative–conductive porous fin with temperature dependent properties, Energy Conv. Management 111 (2016) 279–288, doi:10.1016/j.enconman.2015.12.054.
[23] M. Turkyilmazoglu, Exact heat-transfer solutions to radial fins of general profile, J. Thermophys. Heat Transf. 30 (2015) 1–5, doi:10.2514/1.T4555.
[24] M. Turkyilmazoglu, Thermal management of parabolic pin fin subjected to a uniform oncoming airflow: optimum fin dimensions, J. Therm. Anal. Calorimetry 143 (2021) 3731–3739, doi:10.1007/s10973-020-10382-x.
[25] F.P. Incropera, D.P. DeWitt, T.L. Bergman, A.S. Levine, Fundamentals of Heat and Mass Transfer, 6th Ed., John Wiley & Sons, 2006.
[26] A. Jain, M. Parhizi, L. Zhou, G. Krishnan, Imaginary eigenvalues in multilayer one-dimensional thermal conduction problem with linear temperature-dependent heat generation, Int. J. Heat Mass Transf. 170 (2021) 120993 1-10, doi:10.1016/j.ijheatmasstransfer.2021.120993.
[27] A. Jain, S. McGinty, G. Pontrelli, L. Zhou, Theoretical modeling of endovascular drug delivery into a multilayer arterial wall from a drug-coated balloon, Int. J. Heat Mass Transf. 187 (2022) 122572 1-17, doi:10.1016/j.ijheatmasstransfer.2022.122572.
[28] E.B. Nauman, Chemical Reaction Design, Optimization and Scaleup, 2nd Ed, John, Wiley & Sons, Hoboken, NJ, 2008 ISBN: 9780470282069.
[29] E. Augeraud-Véron, C. Choquet, É. Comte, Optimal control for a groundwater pollution ruled by a convection–diffusion–reaction problem, J. Optimiz. Theory & Appl. 173 (2017) 941–966, doi:10.1007/s10957-016-1017-8.
[30] M. Abramowitz, I. Stegun, Handbook of Mathematical Functions, United States Department of Commerce National Bureau of Standards, 1964.